Preparation and Thermal Properties of Hybrid Nanocomposites of Poly(methyl methacrylate)/Octavinyl Polyhedral Oligomeric Silsesquioxane Blends

Yan Feng,[1,2] Yong Jia,[1,3] Hongyao Xu[1,2]

[1]*College of Material Science and Engineering and State Key Laboratory for Modification of Chemical Fibers and Polymeric Materials, Donghua University, Shanghai 201620, People's Republic of China*
[2]*School of Chemistry and Chemical Engineering, Anhui University, Hefei 230039, People's Republic of China*
[3]*Pharmaceutical Department, Anhui Traditional Chinese Medical College, Hefei 230031, People's Republic of China*

Received 28 June 2007; accepted 21 August 2008
DOI 10.1002/app.29240
Published online 2 December 2008 in Wiley InterScience (www.interscience.wiley.com).

ABSTRACT: A series of poly(methyl methacrylate) (PMMA)/octavinyl polyhedral oligomeric silsesquioxane (POSS) blends were prepared by the solution-blending method and characterized with Fourier transform infrared, X-ray diffraction, transmission electron microscopy, differential scanning calorimetry, and thermogravimetric analysis techniques. The glass-transition temperature (T_g) of the PMMA–POSS blends showed a tendency of first increasing and then decreasing with an increase in the POSS content. The maximum T_g reached 137.2°C when 0.84 mol % POSS was blended into the hybrid system, which was 28.2°C higher than that of the mother PMMA. The X-ray diffraction patterns, transmission electron microscopy micrographs, and Fourier transform infrared spectra were employed to investigate the structure–property relationship of these hybrid nanocomposites and the T_g enhancement mechanism. The results showed that at a relatively low POSS content, POSS as an inert diluent decreased the interaction between the dipolar carbonyl groups of the homopolymer molecular chains. However, a new stronger dipole–dipole interaction between the POSS and the carbonyl of PMMA species formed at the same time, and a hindrance effect of nanosize POSS on the motion of the PMMA molecular chain may have played the main role in the T_g increase of the hybrid nanocomposites. At relatively high POSS concentrations, the strong dipole–dipole interactions that formed between the POSS and carbonyl groups of the PMMA gradually decreased because of the strong aggregation of POSS. This may be the main reason for the resultant T_g decrease in these hybrid nanocomposites. © 2008 Wiley Periodicals, Inc. J Appl Polym Sci 111: 2684–2690, 2009

Key words: blends; nanocomposites; thermal properties

INTRODUCTION

With the rapid growth of nanoscale technologies, the investigation of inorganic–organic nanocomposites based on the hybridization of inorganic materials and polymers on a molecular scale has increased dramatically because of their novel properties in calorifics, mechanics, optics, electromagnetics, and biology.[1–4] Poly(methyl methacrylate) (PMMA; also called organic glass), a kind of colorless and transparent thermoplastic, has good mechanical strength and erosion resistance. However, its lower thermal stability has limited its applications. Therefore, preparing PMMA/nanoparticle composite materials for the improvement of the thermal stability has attracted great interest from many researchers.[5–10] Polyhedral oligomeric silsesquioxane is a unique macromer; it is a well-defined cluster with an inorganic silica-like core (Si_8O_{12}) surrounded by eight organic corner groups (functional or inert).[11] This nanoparticle itself is an inner inorganic–organic hybrid system at the molecular level, so with respect to other inorganic nanoparticle, it can be easily dispersed into a polymer uniformly as an inorganic particle without further surface modification.

In this study, octavinyl-polyhedral oligomeric silsesquioxane (POSS) was blended with PMMA to prepare new inorganic–organic hybrid nanocomposites, which were characterized with Fourier transform infrared (FTIR), X-ray diffraction (XRD), transmission electron microscopy (TEM), differential scanning calorimetry (DSC), and thermogravimetric analysis (TGA) techniques. XRD, TEM, and FTIR

Correspondence to: H. Xu (hongyaoxu@163.com).
Contract grant sponsor: National Natural Science Fund of China; contract grant numbers: 90606011 and 50472038.
Contract grant sponsor: Ph.D. Program Foundation of the Ministry of Education of China; contract grant number: 20070255012.
Contract grant sponsor: Program of Introducing Talents of Discipline to Universities; contract grant number: 111-2-04.
Contract grant sponsor: Shanghai Leading Academic Discipline Project; contract grant number: B603.

spectra were employed to investigate the structure–property relationship of these blend systems, and the glass-transition temperature (T_g) enhancement mechanism was examined in detail.

EXPERIMENTAL

Materials

POSS monomers were synthesized according to the procedures described in ref. 12. Methyl methacrylate was purchased from Aldrich (St. Louis, MO), distilled from calcium hydride under reduced pressure before use, and stored in sealed ampules in a refrigerator. Azobisisobutyronitrile (AIBN), purchased from Shanghai Chemical Reagent Co. (Shanghai, China), was refined in heated ethanol and kept in a dried box. Spectroscopy-grade tetrahydrofuran (THF) and 1,4-dioxane, also purchased from Shanghai Chemical Reagent Co., were dried over 4-Å molecular sieves and distilled from sodium benzophenone ketyl immediately before use. All other solvents were used as received.

Polymerization

The polymerization reactions were carried out under nitrogen protection with a vacuum-line system. The polymer used in this study, PMMA with a weight-average molecular weight (M_w) of 29, 500 g/mol and a polydispersity index [PDI; i.e., weight-average molecular weight/number-average molecular weight (M_w/M_n)] of 2.59 as measured by gel permeation chromatography, was synthesized by free-radical polymerization in 1,4-dioxane at 70°C under a nitrogen atmosphere with AIBN as the initiator for 8 h. The product was purified by dissolution in THF, reprecipitation from methanol, and then drying in a vacuum oven at 40°C to a constant weight.

Solution blending and sample preparation

Blends were prepared by the dissolution of PMMA and POSS in THF at room temperature. In a typical process, 9.916 mmol of PMMA and 0.084 mmol of POSS monomer were dissolved in 10 mL of THF and stirred for 30 min. The solution was allowed to evaporate slowly at 25°C for 24 h on a Teflon plate and was dried in a vacuum oven at 90°C to a constant weight to ensure total elimination of the solvent. The dried films were then ground into powders.

Instrumentation

FTIR spectra were measured with a spectral resolution of 1 cm^{-1} on a Nicolet Avatar 320 FTIR spectrophotometer (Nicolet Analytical Instruments, Madison, WI) in the transmission mode with KBr disks or pellets at room temperature. M_w, M_n, and PDI were determined with a Waters 510 gel permeation chromatograph (Waters Chromatography Division, Millipore Corp., Milford, MA). DSC was performed on a DSC 9000 (Dupont, Boston, MA) equipped with a liquid nitrogen cooling accessory unit under a continuous nitrogen purge (50 mL/min). The scan rate was 20°C/min within the temperature range of 20–130°C. The sample was quickly cooled to 0°C after the first scan, and it was subsequently reheated from 20 to 250°C at 10°C/min. T_g was taken as the midpoint of the specific heat increment. TGA was carried out with a TGA 2050 thermogravimetric analyzer (TA Instruments, New Castle, DE) with a heating rate of 20°C/min from 25 to 700°C under a continuous nitrogen purge (100 mL/min). The thermal degradation temperature was defined as the temperature of 5% weight loss. XRD data were recorded with a Bruker AXS D8 Discover instrument (Bruker-AXS GmbH, Karlsruhe, Germany) with a general area detector diffraction system powder diffractometer and a charged coupling device camera detector. Cu Kα radiation was generated at 40 kV and 40 mA. TEM micrographs were obtained with a JEM-100SX instrument (JEOL Ltd., Tokyo, Japan) operated at 100 kV. The specimens were embedded in an epoxy resin, and ultrathin sections (~ 60 nm) were cut and examined.

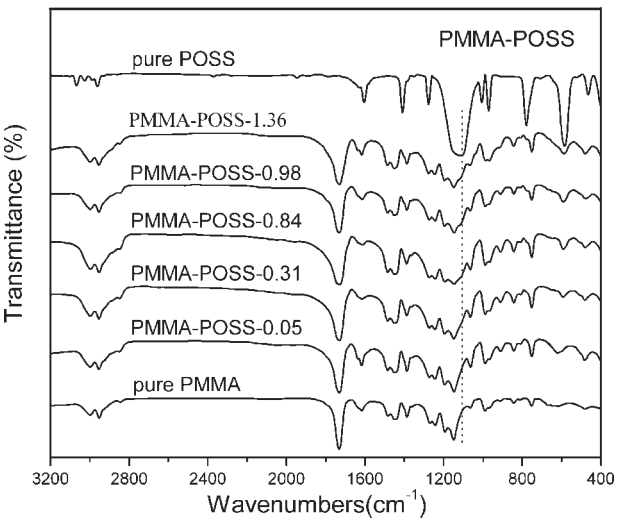

Figure 1 FTIR spectra of pure POSS, PMMA, and PMMA–POSS blends.

RESULTS AND DISCUSSION

FTIR spectra

FTIR was used to check the structures of the resulting PMMA–POSS blends. Figure 1 shows the FTIR spectra of PMMA–POSS blends as well as pure

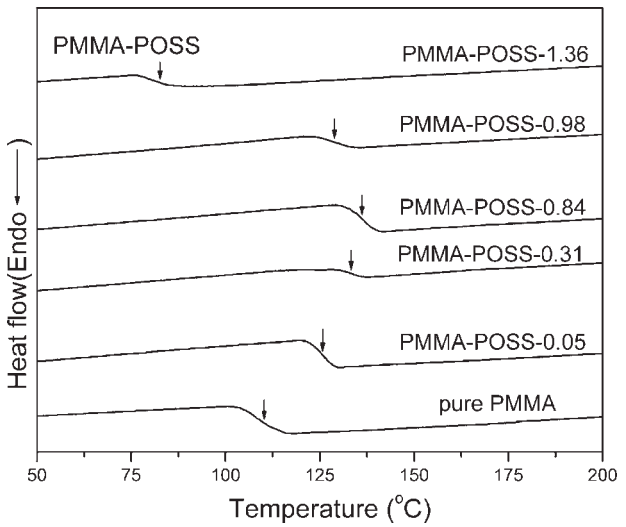

Figure 2 DSC thermograms of PMMA and PMMA–POSS blends.

POSS and PMMA for comparison. The pure POSS shows a strong and symmetric Si—O—Si stretching absorption band at $\sim$ 1109 cm^{-1}, which is the characteristic absorption peak of silsesquioxane cages. The PMMA shows two characteristic absorptions at 1732 and 1148 cm^{-1}, which are assigned to the carbonyl stretching vibration and the strong C—O—C stretching absorption, respectively. The IR spectra of the PMMA–POSS blends are very similar to that of PMMA, except that a sharp and strong Si—O—Si stretching peak appears at 1109 cm^{-1} in all PMMA–POSS blends. The consistent presence of this Si—O—Si stretching peak at 1109 cm^{-1} confirms that the POSS cage is truly present in the resulting hybrid nanocomposites.

DSC and TGA thermograms

The DSC and TGA techniques were employed to investigate the thermal properties of the PMMA–POSS blends. Figure 2 shows the DSC thermograms of PMMA and PMMA–POSS blends, and Table I shows their thermal properties. The PMMA homopolymer has a T_g at 109.0°C. When 0.05 mol % POSS is blended into the PMMA polymers, T_g increases to 125.7°C. When 0.31 or 0.84 mol % POSS is mixed with the PMMA polymers, T_g increases to 134.4 or 137.2°C, respectively. This proves that the incorporation of a relatively small amount of POSS macromers into the homopolymers can effectively improve T_g of the mother polymers. However, T_g of the PMMA–POSS blend decreases with a further increase in the POSS content. For example, when 0.98 mol % POSS is blended into the polymer system, T_g at 128.8°C is observed, which is lower than T_g of PMMA–POSS-0.84 but still 19.8°C higher than that of the mother PMMA. When the molar percentage of POSS in the hybrid nanocomposite reaches 1.36%, the PMMA–POSS blend shows a low T_g at 82.6°C. As a result, the observed T_g values of the PMMA–POSS blends show a tendency of first increasing and then decreasing with the increase in the POSS content. When the molar percentage of POSS in the hybrid nanocomposite is lower than 0.98%, T_g of the PMMA–POSS blend is higher than that of the mother PMMA, and T_g reaches the maximum when the molar percentage of POSS is 0.84%. However, when the molar percentage of POSS in the blends reaches 1.36%, T_g of the hybrid nanocomposite is lower than that of the neat PMMA. This shows that the incorporation of a relatively large amount of POSS macromers into the homopolymers does not increase T_g of the mother polymer but actually reduces its T_g because of the strong aggregation of POSS particles in the nanocomposites.

Figure 3 shows the TGA thermograms of various PMMA–POSS blends and pure PMMA. The thermal decomposition temperature (T_d) of each weight-loss step and the char yield are recorded in Table I. The PMMA homopolymer has four weight-loss steps and has no remnant when the temperature reaches 500°C. When the molar percentage of POSS in the hybrid nanocomposite is less than 0.98%, the blend has only three weight-loss steps, and T_d is in the

TABLE I
Effect of the POSS Ratio on the Properties of PMMA–POSS Blends

Sample	PMMA (mol %)	POSS (mol %)	T_g (°C)[a]	T_d (°C)[b]				Char (%)[c]
				Step 1	Step 2	Step 3	Step 4	
1	100.00	0.00	109.0	182.3	218.5	281.5	348.1	0
2	99.95	0.05	125.7	131.6	/	283.5	337.8	0
3	99.69	0.31	134.4	130.9	/	280.3	352.5	1.2
4	99.16	0.84	137.2	130.9	/	281.9	349.1	1.5
5	99.02	0.98	128.4	129.8	/	280.1	348.1	1.5
6	98.64	1.36	82.6	122.1	221.6	281.9	348.1	3

[a] The data were gathered by DSC during the second melt with a heating and cooling rate of 10°C/min.
[b] The data were determined by TGA at the thermal decomposition temperature of each weight-loss step.
[c] The data were the char residues based on the TGA curve at 500°C.

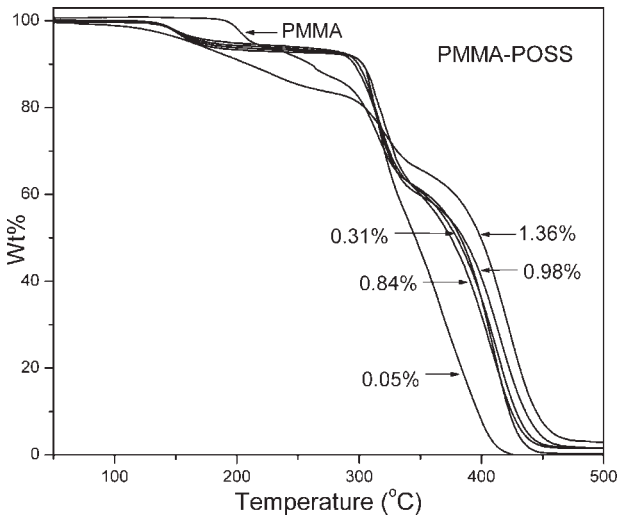

Figure 3 TGA thermograms of PMMA and PMMA–POSS blends.

range of 129.8–131.6, 280.1–283.5, and 337.8–352.5°C, respectively. When the molar percentage of POSS reaches 1.36%, similar to that of the PMMA homopolymer, the nanocomposite also has four loss steps. Comparing the T_d values of the PMMA homopolymer and the nanocomposite, we find that T_d of the nanocomposite is reduced in the relatively low temperature area but slightly increased in the relatively high temperature area. Furthermore, the char yield of the hybrid nanocomposite increases with the increase in the POSS content. These facts indicate that the thermal degradation has been partially restrained at the higher temperature in the PMMA–POSS blends because of the incorporation of the POSS nanoparticles.

T_g change mechanism

In our previous study, we reported pendent poly (acetoxylstyrene-*co*-isobutylstyryl polyhedral oligomeric silsesquioxane), poly(vinylpyrrolidone-*co*-isobutylstyryl polyhedral oligomeric silsesquioxane), and star poly(acetoxystyrene-*co*-octavinyl polyhedral oligomeric silsesquioxane) hybrid nanocomposites synthesized by radical polymerization.[13–15] The DSC and TGA measurements reveal that the incorporation of POSS into polymers can improve the thermal properties of polymeric materials. The T_g values of these nanocomposites first decrease and then increase with the increase in the POSS content. The POSS is covalently bonded to the polymer and can be distributed uniformly in the copolymerized nanocomposites. In the pendent and star copolymerized nanocomposites, POSS acts as an inert diluent to reduce T_g at a relatively low POSS content. With an increase in the POSS content, both the dipole–dipole interaction between the POSS and polymer and the molecular motion hindrance from nanosize POSS contribute to the increase in T_g. In this study, the T_g values of the PMMA–POSS blends first increase and then decrease with the increase in the POSS content; this is just the opposite of the copolymerized nanocomposites. The reason may be that the nanocomposites in this experiment were synthesized by physical blending, and the dispersion of POSS in the nanocomposites may be the main factor that leads to the T_g increase for the hybrid materials. To verify this hypothesis, XRD and TEM were used to characterize the miscibility of the PMMA–POSS blends.

XRD analysis

XRD was used to further characterize the dispersion of the PMMA–POSS blends. Diffraction patterns of the pure PMMA, POSS, and PMMA–POSS blends are shown in Figure 4. The X-ray powder pattern of POSS shows three main characteristic diffraction peaks at 9.8, 20.1, and 29.9° (2θ). These values are typical for the crystal structure of POSS. A broad amorphous diffraction peak of PMMA is at ~ 14.1° (2θ). In each case, the PMMA–POSS-0.09 and PMMA–POSS-0.31 diffraction patterns have only a broad amorphous peak at ~ 14.1° (2θ), corresponding to the amorphous PMMA matrix peak. The appearance of this broad amorphous peak means that no significant aggregation happens when the molar percentage of POSS is 0.31% or lower, PMMA and POSS are relatively evenly distributed in the nanocomposites, and the nanosize POSS can hinder the motion of the PMMA molecular chain and make a contribution to the T_g increase. When the POSS molar percentage reaches 0.84%, a new peak matching the peak of POSS at 9.8° appears and becomes

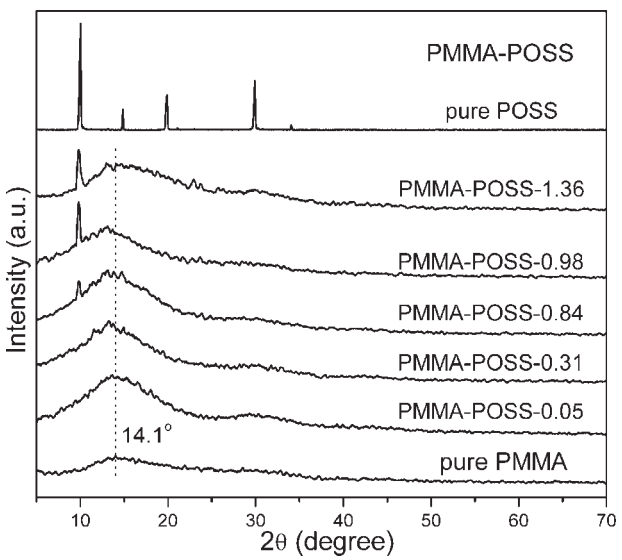

Figure 4 XRD patterns of POSS, PMMA, and PMMA–POSS blends.

more prominent for PMMA–POSS-0.98 and PMMA–POSS-1.36. The appearance of this characteristic peak in the PMMA–POSS blend diffraction patterns shows that the POSS nanoparticles have aggregated in the blend and that the degree of aggregation increases with the increase in the POSS content. The aggregated POSS cluster results in a T_g decrease.

If indeed POSS particles are distributed throughout the matrix, we should observe a shift in the location of the amorphous peak of PMMA ($2\theta = 14.1^\circ$), and the POSS nanoparticles will be expected to push polymer chains apart and shift the amorphous peak to the smaller angle.[10] As expected, the POSS present in the blends tends to slightly shift the locations of the PMMA matrix peaks to smaller 2θ values in Figure 4. When 0.05 mol % POSS is blended into the PMMA polymers, the 2θ value decreases to 13.73°. When 0.31 or 0.84 mol % POSS is mixed with the PMMA polymers, the 2θ value further decreases to 13.34 or 13.19°, respectively. Even when the molar percentage of POSS reaches 0.98 or 1.36%, the 2θ value still keeps decreasing to 13.13 or 12.98°. All the 2θ values are smaller than that of pure PMMA ($2\theta = 14.1^\circ$), indicating that the POSS nanoparticles have penetrated between the PMMA chains and formed a sort of novel inorganic–organic hybrid nanocomposite.

An analysis of the XRD patterns of the blend systems shows that significant aggregation of the POSS becomes apparent when the molar percentage of POSS reaches 0.84%. In combination with the DSC results, we can realize that the dispersion of POSS in the PMMA–POSS blends shows an obvious effect on the thermal properties of the nanocomposite. At a relatively low POSS content (<0.84 mol %), the POSS nanoparticles can distribute relatively uniformly in the nanocomposites, resulting in an increase in T_g. At a relatively high POSS content (>0.84 mol %), the aggregation becomes dominant and leads to a decrease in T_g.

TEM analysis

For further confirming the POSS distribution in the nanocomposites, the PMMA–POSS nanocomposites at three different POSS concentrations were characterized with TEM. As can be seen in Figure 5, at relatively low POSS contents such as 0.31 mol %, almost no significant aggregated particles of POSS were observed [Fig. 5(a)]. However, at relatively high POSS concentrations such as 0.84 mol %, only small amounts of aggregated particles of POSS were found. Significant aggregation was found and the particle diameter was about 5–20 nm when the POSS concentration reached 0.98 mol % [Fig. 5(b)]; the aggregated particles showed a further aggrandizement tendency with an increase in the POSS concentration, such as 1.36 mol %, in the blend [Fig. 5(c)]. The results are in good agreement with those of XRD, further confirming that at a relatively high POSS content, POSS aggregation happens and

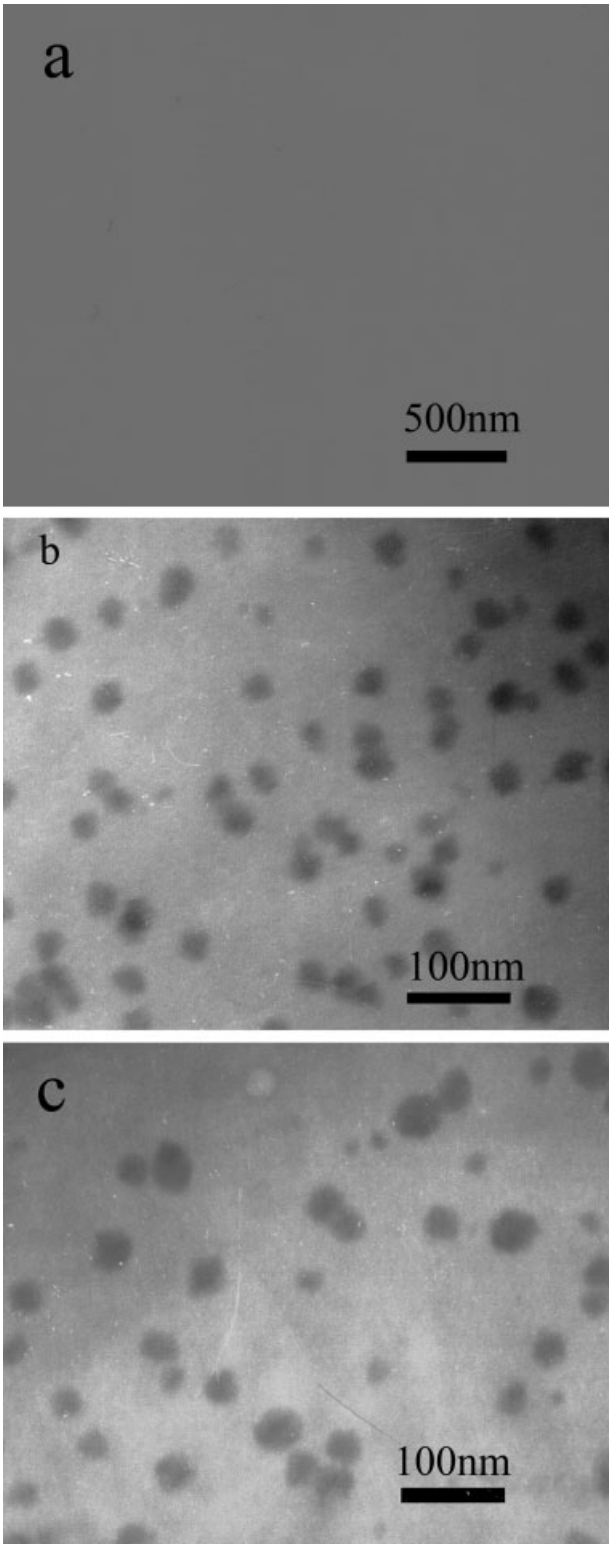

Figure 5 TEM micrographs of PMMA–POSS blends with three different POSS molar contents: (a) 0.31, (b) 0.98, and (c) 1.36 mol %.

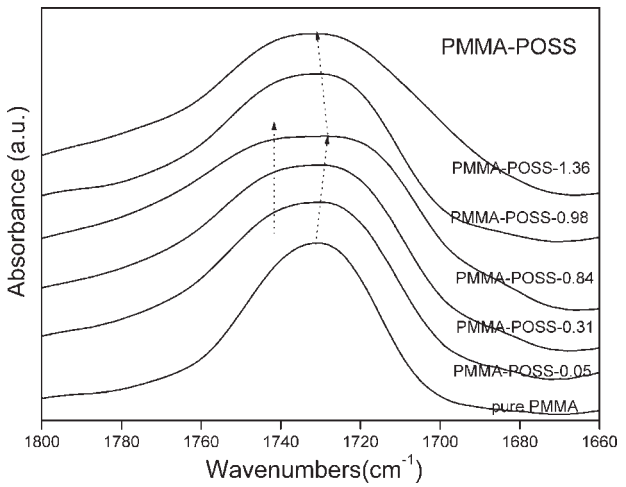

Figure 6 Expanded FTIR spectra ranging from 1800 to 1660 cm^{-1} for PMMA and PMMA–POSS blends.

the aggregation effect increases with the POSS concentration increasing.

FTIR analysis

To further reveal the T_g change mechanism involved in the PMMA–POSS blends, the characterization of their FTIR spectra was carried out. Figure 6 shows the expanded FTIR spectra of pure PMMA and various PMMA–POSS blends ranging from 1800 to 1660 cm^{-1}. The pure PMMA shows the characteristic carbonyl absorption at 1732 cm^{-1}; however, when POSS is blended into PMMA, the carbonyl absorption begins to shift to a lower wave number. For example, when 0.31 mol % POSS is blended into PMMA (PMMA–POSS-0.31), the carbonyl absorption shifts to 1729 cm^{-1}, and there is a trend in which the carbonyl absorption peak shifts toward a lower wave number with an increase in the POSS content. In addition, the band is obviously widened when POSS is blended into PMMA, and a stronger shoulder peak at a higher frequency ($\sim$ 1750 cm^{-1}) is found when POSS is incorporated into PMMA. It appears that there is a new stronger dipole–dipole interaction existing between POSS and the carbonyl of the PMMA species, and the interaction becomes stronger with an increase in the POSS content, which is probably responsible for the positive contribution to the T_g increase of the hybrid nanocomposite at the lower POSS content. However, when the POSS content is further increased to 0.98 mol %, this maximum absorption peak of the carbonyl group shifts slightly toward a higher frequency gradually and further shifts toward a higher wave number with an increase in the POSS content in the PMMA–POSS blends. For instance, the carbonyl maximum absorption peak of PMMA at 1732 cm^{-1} decreases to 1728 cm^{-1} for PMMA–POSS-0.84 but increases to 1730 cm^{-1} for PMMA–POSS-0.98 and 1733 cm^{-1} for PMMA–POSS-1.36. Furthermore, the shoulder peak becomes inconspicuous when the POSS content is more than 0.98 mol %, showing that the dipole–dipole interaction between PMMA and POSS decreases in the PMMA–POSS blends, and this may result from the POSS aggregation. This is consistent with the results of XRD patterns and TEM micrographs.

Cheam and Krimm[16] studied the relationship between the dipole interaction potential (V_{dd}) and the FTIR vibration frequency shift ($\Delta\upsilon_i$), which is expressed as follows:

$$\Delta\upsilon_i = \frac{V_{dd}}{hc} \quad (1)$$

h is Planck's constant and c is the velocity of light.

The frequency shift is related to the strength of the dipole interaction. The absorbance frequency will increase with the enhancement of the dipole interaction and decrease with the weakening of the dipole interaction. Painter et al.[17] studied the interaction potential between two dipoles, A and B, which is expressed in the following formula:

$$V_{dd} = -\mu_A\mu_B[\hat{e}_A\,\hat{e}_B - 3(\hat{e}_A \bullet r_{AB})(\hat{e}_A - r_{AB})]/r_{AB}^3 \quad (2)$$

where μ is the value of dipole moment, $\hat{e}$ is a unit vector describing the direction of the dipole moment and r_{AB} is the distance between the centers of the dipoles. From formula 2, we know that the increase in the distance between the centers of the dipoles will lead to a drop in the dipole interaction. Therefore, according to this theory and the FTIR spectra, we can well explain the T_g change of the nanocomposites. In our previous work on POSS-containing nanocomposite,[13,15] we found that, when a relatively small amount of POSS is chemically incorporated into poly(4-acetoxystyrene) POSS acts as a diluent, enlarging the distance between the dipolar carbonyl groups of homopolymer molecular chains and resulting in a decrease in their dipole–dipole interaction. Simultaneously, the nanoscale POSS also hinders molecular chain motion. Therefore, the dilution effect of POSS may play a main role in reducing T_g, and similar results were also found in our previous work.[13–15] With a further increase in the POSS content, distance r_{AB} between the POSS and the polar carbonyl group of the polymer chain is shortened; this results in an increase in the dipole–dipole interaction between the POSS and carbonyl with the increase in the POSS content. Therefore, the dipole–dipole interaction between the POSS and the polar carbonyl of poly(4-acetoxystyrene) plays a main role at a relatively high POSS content, resulting in a T_g increase.

In the PMMA–POSS blend, at a relatively low POSS content, the inert diluent, POSS, reduces the

interaction between the dipolar carbonyl groups of homopolymer molecular chains; this has been confirmed by FTIR spectra. However, a new stronger dipole–dipole interaction between the POSS and the carbonyl of the PMMA species and a hindrance effect of nanosize POSS on the motion of the PMMA molecular chain may be responsible for the positive contribution to the T_g increase of the hybrid nanocomposite. At a relatively high POSS concentration, the new stronger dipole–dipole interaction between the POSS and the carbonyl of PMMA species gradually decreases because of a strong aggregation effect of POSS, which may be the main reason for the T_g decrease of the hybrid nanocomposite. Furthermore, when the molar percentage of POSS in the blends reaches 1.36%, T_g of the hybrid nanocomposite is lower than that of the pure PMMA. This shows that when the POSS nanoparticles aggregate to a certain degree, both the dipole–dipole interaction between the POSS and the carbonyl of the PMMA species and the hindrance effect of nanosize POSS on the motion of the PMMA molecular chain will gradually be diminished. Moreover, the aggregated POSS cluster will weaken the dipole–dipole interaction between PMMA chains and the self-association interaction of PMMA molecules. They may be the main reasons for T_g being lower than that of the neat polymer. This is consistent with the results of FTIR, XRD, and TEM. Therefore, the observed T_g values of the PMMA–POSS blends show a tendency of first increasing and then decreasing with an increase in the POSS content.

CONCLUSIONS

Hybrid nanocomposites of PMMA–POSS containing various POSS contents were prepared by a solution blending method. The results show that, at a relatively low POSS content, a new stronger dipole–dipole interaction between the POSS and the carbonyl of PMMA species and a hindrance effect of nanosize POSS on the motion of the PMMA molecular chain result in a T_g increase of the hybrid nanocomposites. At a relatively high POSS concentration, the dipole–dipole interactions that form between the POSS and the carbonyl of the PMMA species gradually decrease because of a strong aggregation effect of POSS, and this results in a T_g decrease of the hybrid nanocomposite.

References

1. Zhang, C.; Babonneau, F.; Bonhomme, C.; Laine, R. M.; Soles, C. L.; Hristov, H. A.; Yee, A. F. J Am Chem Soc 1998, 120, 8380.
2. Zheng, L.; Farris, R. J.; Coughlin, E. B. Macromolecules 2001, 34, 8034.
3. Wang, J. F.; Xu, H. Y.; Bao, L. Polym Mater Sci Eng 2005, 21, 10.
4. Cheng, W. D.; Xiang, K. H.; Pandey, R.; Pernisz, U. C. J Phys Chem B 2000, 104, 6737.
5. Koh, K.; Sugiyama, S.; Morinaga, T.; Ohno, K.; Tsujii, Y.; Fukuda, T.; Yamahiro, M.; Iijima, T.; Oikawa, H.; Watanabe, K.; Miyashita, T. Macromolecules 2005, 38, 1264.
6. Kopesky, E. T.; McKinley, G. H.; Cohen, R. E. Polymer 2006, 47, 299.
7. Kopesky, E. T.; Haddad, T. S.; Cohen, R. E.; McKinley, G. H. Macromolecules 2004, 37, 8992.
8. Chen, M.; Zhou, S.; You, B.; Wu, L. Macromolecules 2005, 38, 6411.
9. Huang, C. F.; Kuo, S. W.; Lin, F. J.; Huang, W. J.; Wang, C. F.; Chen, W. Y.; Chang, F. C. Macromolecules 2006, 39, 300.
10. Kopesky, E. T.; Haddad, T. S.; McKinley, G. H.; Cohen, R. E. Polymer 2005, 46, 4743.
11. Baney, R. H.; Itoh, M.; Sakakibara, A.; Suzuki, T. Chem Rev 1995, 95, 1409.
12. Harrison, P. G.; Hall, C.; Kannengiesser, R. Main Group Met Chem 1997, 20, 515.
13. Xu, H. Y.; Kuo, S. W.; Lee, J. S.; Chang, F. C. Macromolecules 2002, 35, 8788.
14. Xu, H. Y.; Kuo, S. W.; Lee, J. S.; Chang, F. C. Polymer 2002, 43, 5117.
15. Xu, H. Y.; Yang, B. H.; Wang, J. F.; Guang, S. Y.; Li, C. Macromolecules 2005, 38, 10455.
16. Cheam, T. C.; Krimm, S. Chem Phys Lett 1984, 107, 613.
17. Painter, P. C.; Pehlert, G. J.; Hu, Y.; Coleman, M. M. Macromolecules 1999, 32, 2055.